Acute kidney injury model established by systemic glutathione depletion in mice

Journal:	*Journal of Applied Toxicology*
Manuscript ID	JAT-18-0403.R2
Wiley - Manuscript type:	Research Article
Date Submitted by the Author:	n/a
Complete List of Authors:	Matsubara, Akiko; Nagoya University Graduate School of Medicine, 65 Tsurumai-cho, Showa-ku, Nagoya, 466-8550, Japan. Oda, Shingo; Nagoya University Graduate School of Medicine, Department of Drug Safety Sciences Jia, Ru; Nagoya University Graduate School of Medicine, 65 Tsurumai-cho, Showa-ku, Nagoya, 466-8550, Japan. Yokoi, Tsuyoshi; Nagoya University Graduate School of Medicine, Department of Drug Safety Sciences
Keywords:	acute kidney injury, animal model, BSO, glutathione, myoglobin.

Acute kidney injury model established by systemic glutathione depletion in mice

Akiko Matsubara, Shingo Oda, Ru Jia, and Tsuyoshi Yokoi*

Department of Drug Safety Sciences, Division of Clinical Pharmacology, Nagoya University Graduate School of Medicine, 65 Tsurumai-cho, Showa-ku, Nagoya, 466-8550, Japan.

amatsubara@med.nagoya-u.ac.jp (A. Matsubara)
shingo61@med.nagoya-u.ac.jp (S. Oda)
newjiaru@med.nagoya-u.ac.jp (R. Jia)
tyokoi@med.nagoya-u.ac.jp (T. Yokoi)

*** Corresponding author:** Tsuyoshi Yokoi, Ph.D.
Department of Drug Safety Sciences,
Nagoya University Graduate School of Medicine, 65 Tsurumai-cho, Showa-ku, Nagoya, 466-8550, Japan.
E-mail: tyokoi@med.nagoya-u.ac.jp
Tel: +81-52-744-2110, Fax: +81-52-744-2114

Funding information

Grant-in-Aid for Scientific Research (A) (No. 16H02616) from the Japan Society for the Promotion of Science.

Key words: acute kidney injury; animal model; BSO; glutathione; myoglobin.

Abbreviations: ALT, alanine aminotransferase; AST, aspartate aminotransferase; ath, *Arabidopsis thaliana*; BSO, L-buthionine-(*S,R*)-sulfoximine; BUN, blood urea nitrogen; CPK, creatine phosphokinase; CRE, creatinine; Gapdh, glyceraldehyde-3-phosphate dehydrogenase; GSH, glutathione; H&E, hematoxylin-eosin; Ho, heme oxygenase; Lcn, lipocalin; Mb, myoglobin; miRNA, microRNA; Ngal, neutrophil gelatinase-associated lipocalin; RT, reverse transcription; Tnfα, tumor necrosis factor alpha; Xirp, xin actin-binding repeat containing.

Abstract

Glutathione (GSH) is one of the most extensively studied tripeptides. The roles for GSH in redox signaling, detoxification of xenobiotics, and antioxidant defense, have been investigated. A drug-induced rhabdomyolysis mouse model was recently established in L-buthionine-(*S,R*)-sulfoximine (BSO), a GSH synthesis inhibitor, -treated normal mice by co-administration of antibacterial drug and statin. In these models, mild kidney injury was observed in the BSO only-treated mice. Therefore, in this study, we studied the kidney injury in GSH-depleted mouse. BSO was intraperitoneally administered twice a day for 7 days to normal mice. The maximum level of plasma creatine phosphokinase (CPK) (351,487 ± 53,815 U/L) was shown on day 8, and that of aspartate aminotransferase (AST) was shown on day 6. Increased levels of blood urea nitrogen (BUN), plasma creatinine (CRE), urinary kidney injury molecule (KIM-1), and urinary CRE were observed. An increase of mRNA expression level of renal lipocalin 2/neutrophil gelatinase-associated lipocalin (Lcn2/Ngal) was observed. Degeneration and necrosis in the skeletal muscle and high concentrations of myoglobin (Mb) in blood (347-203,925 ng/mL) and urine (2.5-68,583 ng/mL) with large interindividual variability were shown from day 5 of BSO administration. Mb-stained regions in the renal tubule and renal cast were histologically observed. In this study, the GSH-depletion treatment established an acute kidney injury (AKI) mouse model due to Mb release from the damaged skeletal muscle. This mouse model would be useful for predicting potential AKI risks in non-clinical drug development.

1. INTRODUCTION

Glutathione (γ-glutamyl-cysteinyl-glycine; GSH) is the most abundant low-molecular-weight non-protein thiol, consisting of glycine, glutamic acid, and cysteine. GSH plays important roles in redox signaling, detoxification of xenobiotics, antioxidant defense, nutrient metabolism, regulation of cell proliferation, apoptosis, and immune responses (Lu, 2013, Wu et al., 2004). GSH conjugates with reactive intermediates derived from exogenous substances such as drugs and environmental chemicals, and protects endogenous proteins and nucleic acids (Lu, 1999). GSH depletion contributes to oxidative stress, which plays a key role in the pathogenesis of many diseases, including seizures, cystic fibrosis, hypertension, diabetes, and degenerative diseases (Ames et al., 1993: Vaziri et al., 2000: Lu, 2013). The pathogenic mechanisms of GSH at the molecular level have been well studied.

L-buthionine-(*S,R*)-sulfoximine (BSO) is a representative inhibitor of GSH synthesis, and has been reported to inhibit γ-glutamyl-cysteine synthetase (γ-GCS), a rate-limiting enzyme of GSH synthesis, specifically and irreversibly (Griffith, 1982). BSO showed gene changes similar to *in vivo*, naturally decreasing the profile of GSH content in mice (Kiyosawa et al., 2004 & 2007). Therefore, BSO is proper for investigating the GSH detoxifying mechanism and function.

In the normal state, GSH levels in the kidneys, skeletal muscle, and heart are lower than that of liver, lung, and spleen in mice (Watanabe et al., 2003). In addition, GSH contents in kidney and skeletal muscle can be reduced more rapidly and more potently than the liver, heart, lung, and spleen by the BSO treatment in mice (Watanabe et al., 2003).

We previously reported several evaluation systems on drug-induced liver/kidney injury by using BSO-treated rodents (Shirai et al., 2017; Iida et al., 2015; Iwamura et

al., 2016). In our recent studies, was established in BSO-treated normal mice by co-administration of ciprofloxacin (a new quinolone antibacterial drug) and atorvastatin (a blood cholesterol lowering drug) (Matsubara et al., 2018). In these models, mild kidney injury was observed in the BSO only-treated control mice. Therefore, in this study, we intended to clarify the effect of GSH depletion in the normal mice. BSO was adopted as a GSH-depleting agent and its effects on skeletal muscle and kidney were studied.

2. MATERIALS AND METHODS

2.1 Chemicals and Reagents

BSO and anti-myoglobin (Mb) antibody produced in rabbit (product #M8648) were purchased from Sigma Aldrich (St. Louis, MO). A Target Retrieval Solution Citrate pH 6 and Dual Link System were purchased from Dako Japan (Tokyo, Japan). RNAiso Plus and SYBR Premix Ex Taq (Tli RNaseH Plus) were obtained from Takara (Ohtsu, Japan). The ReverTra Ace qPCR RT Kit was obtained from Toyobo (Osaka, Japan). The miRNeasy Serum/Plasma Kit was obtained from Qiagen (Valencia, CA). The TaqMan® MicroRNA Reverse Transcription Kit and TaqMan® miRNA Assay including the microRNA specific primer (ath-miR159a, mmu-miR-206-3p, mmu-miR-133b-3p, mmu-miR-208-3p, mmu-miR-122-5p) and TaqMan® Universal Master Mix that does not contain uracil-N glycosylase (UNG) were obtained from Applied Biosystems (Foster City, CA). All primers were synthesized at Hokkaido System Sciences (Sapporo, Japan). A mouse Mb enzyme-linked immunosorbent assay (ELISA) kit was purchased from Life Diagnostics (West Chester, PA). Other chemicals used in this study were the highest grade commercially available.

2.2 Animal treatment and biochemical analyses

Six-week-old male C57BL/6J mice were obtained from Japan SLC (Hamamatsu, Japan). The mice were kept under a 12-hour light/dark cycle (lights on 9:00-21:00) in a controlled environment (temperature 23°C ± 2°C, humidity 55% ± 10%) in the institutional animal facility. The animals were acclimatized before use in the experiments. BSO treatment was performed twice a day (every 12 hours) for 7 days. BSO was dissolved in saline (70 mg/mL) and intraperitoneally (*i.p.*) administered to mice at a dose of 1000 mg/kg. All mice were allowed free access to water. An overnight fasting for 12 hours was conducted every day. After the first BSO treatment, the mice were again allowed access to food *ad libitum*. These procedures were repeated for 7 consecutive days. Twenty-four hours after the last BSO treatment, blood and urine were collected from the inferior vena cava under isoflurane anesthesia, and liver, kidney, and skeletal muscle tissue mainly containing gastrocnemius muscle were collected from day 3. Plasma was separated from blood samples by centrifugation at 4°C at 1600 × g for 10 minutes. The levels of alanine aminotransferase (ALT), aspartate aminotransferase (AST), blood urea nitrogen (BUN), creatinine (CRE), and creatine phosphokinase (CPK) in plasma were measured using Fuji Dri-Chem 4000 (Fujifilm, Tokyo, Japan) according to the manufacturer's instructions. Plasma and urine were diluted with MilliQ water as needed.

Regarding the control sample, throughout the present study, the Day 0 sample as a control group was collected from individuals before BSO treatment. The Day 8 saline sample as a control group was treated with the same dosing volume of saline as BSO. All procedures performed on animals were approved by the Institutional Animal Care Committee of Nagoya University Graduate School of Medicine (No. 29256). All animal experiments were performed in accordance with the guidelines established by the

Institute for Laboratory Animal Research of the Medical School of Nagoya University.

2.3 Histopathological examination

The kidney was fixed in 10% neutral-buffered formalin, and the samples were embedded in paraffin. The skeletal muscle tissue, quick-frozen in liquid nitrogen-cooled isopentane, was embedded in an optimal cuting temperature (OCT) compound (Tissue-Tek, Torrance, CA) and frozen in 2-methylbutane cooled with dry ice. The sections of kidney (4-μm thickness) and skeletal muscle (8-μm thickness) were stained with hematoxylin-eosin (H&E). The stained sections were observed under a microscope for routine pathological examination.

2.4 Measurement of kidney injury molecule-1 (KIM-1) concentration in urine and Mb concentration in plasma and urine by ELISA

KIM-1 concentration in urine was measured using the Mouse TIM-1/KIM-1/HAVCR Immunoassay kit (R&D Systems Inc, Minneapolis, MN) according to the manufacturer's protocol. Absorbance at 450 nm was measured using the TECAN Infinite F 200 PRO (Tecan, Mannedorf, Switzerland). Mb concentration in plasma and urine was measured using the Myoglobin ELISA kit (Life Diagnostics Inc, West Chester, PA) according to the manufacturer's protocol. Plasma and urine were diluted as necessary, and absorbance at 450 nm was measured using the TECAN Infinite F 200 PRO.

2.5 Immunohistochemical examination of Mb

For the detection of Mb in the kidney, the sections of kidney were immunostained with anti-Mb antibody as follows: after dehydration and dexylene, endogenous peroxidase activity was quenched by incubation in 3% H_2O_2/PBS for 15 minutes, then washed

twice with PBS for 5 minutes. Antigen activation was treated with Target Retrieval Solution Citrate pH 6 (Dako, Japan) at 95°C for 20 minutes. After standing at room temperature for 20 minutes, the sections were washed twice with PBS for 5 minutes. Therafter, the sections were incubated with normal goat serum diluted 10-fold with 1% bovine serum albumin (BSA)/PBS at 37°C for 20 minutes. After gentle washing with PBS, the tissue sections were incubated with an anti-Mb (1:500 diluted with 1%BSA/PBS) antibody (Sigma-Aldrich, M8648). After incubation at 37°C for 1 hour, the sections were washed twice with PBS for 5 minutes. The sections were then incubated with Envision Dual Link System (Dako, Japan) at 37°C for 30 minutes. After washing twice with PBS for 5 minutes, diaminobenzidine (DAB) solution was added and color developed at room temperature for 6 minutes. The sections were counterstained with H&E. The stained sections were observed under a microscope for routine pathological examination.

2.6 miRNA and mRNA extraction and real-time reverse transcription-polymerase chain reaction (RT-PCR)

For the plasma miRNA analysis, the plasma samples were mixed with QIAzol Lysis Reagent (Qiagen), and as a spike in control, *Arabidopsis thaliana* (ath)-miR159a was added. Total RNA was extracted using a miRNeasy Serum/Plasma Kit, and RT was performed using a TaqMan®MicroRNA Reverse Transcription Kit according to the manufacturer's instructions. The PCR mixture contained 2.5 μL of product from the RT reaction, TaqMan® Small RNA Assay (miR-206-3p, miR-133b-3p, miR-208-3p, miR122-5p), and TaqMan® Universal PCR Master Mix II (2×) without UNG. Real-time RT-PCR was performed using an Mx3000P (Agilent Technologies, Santa Cruz, CA). The following thermal profile was used: denaturation at 95°C for 10 minutes, followed

by 40 amplification cycles of 95°C for 15 seconds and 60°C for 1 minute. The amplified product was monitored by measuring the increase of the fluorescein amidite (FAM) fluorescence intensity. Information on miRNAs used in this study is shown in Table 1.

RNA from kidney and liver was isolated using RNAiso Plus according to the manufacturer's instructions. The concentration of the RNA sample was quantified using Nano Drop 2000c (Thermo Scientific). RT was performed using a ReverTra Ace qRT-PCR Kit (Toyobo) according to the manufacturer's instructions. The PCR mixture contained 1 μL of template cDNA, SYBR Premix Ex Taq, sense primer, and antisense primer. The mRNA levels of xin actin-binding repeat containing 1 (Xirp1), lipocalin 2/neutrophil gelatinase-associated lipocalin (Lcn2/Ngal), heme oxygenase 1 (Ho-1), monocyte chemotactic protein-1 (Mcp-1), tumor necrosis factor α (Tnfα), interleukin 6 (Il-6), and interleukin-1 beta (Il-1β) were quantified by real-time RT-PCR using an Mx3000P. The following thermal profile was used: denaturation at 95°C for 30 seconds, followed by 40 amplification cycles of 95°C for 5 seconds and 60°C for 30 seconds. The amplified products were monitored directly by measuring the intensity of the SYBR Green I dye that binds to the PCR-amplified double-stranded DNA. The relative mRNA expression levels were calculated using the comparative C_T method with Gapdh as the reference gene. The primer sequences used in this study are shown in Table 2.

2.7 Quantification of GSH and GSSG in liver, skeletal muscle, and kidney

GSH and GSSG concentrations in the liver, skeletal muscle, and kidney were measured using the GSSG/GSH Quantification Kit (Dojindo, Kumamoto, Japan) according to the manufacturer's protocol. In brief, this kit contains masking reagent of GSH. The GSH can be deactivated in the sample by simply adding the masking reagent.

Therefore, GSSG only was detected by 412 nm absorption of DTNB using the enzymatic recycling system. Thus, GSH can be determined by the quantity by subtracting GSSG from the total amount of glutathione. Absorbance at 412 nm was measured using the POWERSCAN®4 (DS Pharma Biomedical, Osaka, Japan).

2.8 Statistical analysis

All values were represented as the mean ± standard error of the mean (SEM). Statistical analysis was performed using JMP Software (JMP Pro, Version 13.0.0, SAS Institute Inc., Cary, NC). Comparisons of two groups were performed using a two-tailed Student's *t*-test. Comparisons of multiple groups were accomplished using the Dunnett's test. Values of $P < 0.05$ were considered statistically significant.

3. Results

3.1 GSH depletion treatment causes severe muscle injury in mice

BSO, a glutathione synthesis inhibitor, was given *i.p.* to male C57BL/6J mice twice a day (every 12 h) for 7 days. Time-dependent changes of CPK and AST levels were measured 12 h after the second daily BSO treatment from day 3, and significant increases in CPK and AST levels were observed compared with the saline-treated control group from day 6 and from day 5, respectively (Figs. 1A and 1B). The maximum level of CPK was shown on day 8 (351,487 ± 53,815 U/L), whereas that of AST was shown on day 6 (9,640 ± 377 U/L). The body weight of BSO-treated mice increased 10% to 15% after a week compared with that of the day 0 (data not shown) The change in body weight was almost the same as that in the saline-treated control group, and there was no significant difference. Plasma levels of miR-206-3p (a biomarker for skeletal muscle-specific expression) and miR-133b-3p (a biomarker for

skeletal muscle and myocardium-specific expression) were significantly increased on day 8 compared with that of the day 0 and day 8 of the saline control group (Figs. 1C and 1D). The plasma miR-208-3p (a biomarker for myocardium-specific expression) level was not significantly changed (data not shown).

In our previous studies (Higuchi *et al*., 2011; Kobayashi *et al*., 2009), we confirmed that the expression profiles of mRNA and protein were similar for the interleukins, chemokines and stress- and inflammation-related proteins. Thus, changes in the mRNA expression levels were mainly investigated in the present study. The mRNA expression levels of muscle Xirp1, a marker for muscle injury, and Ho-1, an oxidative stress marker, in the skeletal muscle were significantly increased on day 8 compared with that on day 0 and day 8 of the saline control group (Figs. 1E and 1F). To evaluate the injury of skeletal muscle histologically, the skeletal muscle tissue of day 8 was stained with H&E. Degradation in the muscle fibers, necrotic cells, and a slight increase in the number of satellite cells in the BSO-treated group were observed compared with the saline-treated control group (Fig. 1G).

3.2 Mb leakage in plasma, urine, and kidney in GSH-depleted mice

Time-dependent changes in Mb level in plasma and urine were measured at 12 hours after the second daily BSO treatment from day 3 (Figs. 2A, and 2B). Mb level in plasma started to increase from day 5, and showed large interindividual differences on day 7 (plasma; 347-203,925 ng/mL) and day 8. The Mb level in urine also started to increase from day 5, and also showed large interindividual differences on day 8 (urine; 2.5 - 68,583 ng/mL). Immunohistochemical evaluation of the kidney showed positively stained Mb regions in the renal tubule and renal cast in the BSO-treated group (Fig. 2C).

3.3 GSH depletion caused kidney injury in mice

Time-dependent changes of plasma BUN and CRE and urinary CRE levels were measured 12 hours after the second daily BSO treatment from day 3. Significant increases in plasma BUN and CRE and urinary CRE levels were observed compared with the saline-treated control group (Figs. 3A, 3B and 3C). Plasma BUN and CRE showed maximum levels on day 8 (Figs. 3A and 3B), whereas urinary CRE showed maximum level on day 7 (1385 ± 1431 mg/dL). Expression levels of mRNA markers for kidney injury, Lcn2/Ngal, and Kim-1, were significantly increased on day 8 compared with that of day 0 and day 8 of the saline control group (Figs. 3D and 3E). Urinary KIM-1 protein showed an increase trend in the BSO-treated samples (Fig. 3F).

To investigate whether oxidative stress, immune-related responses, and apoptosis-related factors are involved in the kidney of the GSH-depleted mouse, the mRNA expression levels of Ho-1, Il-6, Il-1 β, Tnfα and Mcp-1 on day 8 were determined (Fig. 3G to 3K). Expression level of Ho-1 and Il-6 were significantly increased in only the BSO-treated group compared with that of the day 0 and the day 8 of saline control group (Figs. 3G and 3H). Expression level of Il-1β, TNFα and Mcp-1 showed no significant change on day 8 (Figs. 3I, 3J, and 3K). Time-dependent changes of the mRNAs (Lcn2/Ngal, Kim-1, Ho-1, Il-6, Il-1β, Tnfα, and Mcp-1) expression levels in kidney are shown in Supplemental figure 1. Significant increases were observed in mRNA levels of Lcn2/Ngal, Ho-1, and Il-6 on day 8. To evaluate the injury of kidney histologically, the kidney section was stained with H&E. In BSO-treated mice, renal tubular obstruction and vacuolization were observed (Fig. 3L).

3.4 GSH depletion did not cause liver injury

To investigate the effect of GSH depletion treatment on the liver, time-dependent

changes of plasma ALT level were measured 12 hours after the second daily BSO treatment from day 3. A significant increase of plasma ALT level was observed from day 5 compared with the saline-treated control group (Fig. 4A). Expression level of plasma miR-122-5p (a biomarker for liver-specific expression) was not significantly increased on day 8 compared with that of day 0 and day 8 of the saline control group (Fig.4B). Expression levels of liver Ho-1 mRNA were significantly increased on day 8 compared with that of day 0 and the saline control group (Fig.4C), whereas that of Mcp-1 mRNA was not changed. A time-dependent increase of Ho-1 mRNA, not Mcp-1 mRNA, was observed (Supplemental figure 2). To evaluate the injury of liver histologically, the liver section of day 8 was stained with H&E, resulting no change was observed (data not shown).

3.5 Effect of BSO treatment on GSH content in liver, kidney, and skeletal muscle

Total GSH, GSH, GSSG, and GSH/GSSG ratio were measured on day 8 (12 h after the last BSO treatment) (Fig.5). Levels of total GSH, GSH, and GSSG on day 8 in the BSO-treated group were significantly decreased in the liver, kidney, and skeletal muscle compared with those of day 0 and day 8 of the saline control group (Fig. 6). The GSH/GSSG ratio, a marker of oxidative stress, was significantly decreased compared with the day 0 group in the liver, kidney, and skeletal muscle.

4. Discussion

Recently, we established a drug-induced rhabdomyolysis mouse model by co-administration of atorvastatin (a blood cholesterol lowering drug) and ciprofloxacin (an antibacterial drug) (Matsubara *et al*., 2018). GSH depletion by BSO treatment was essential for the establishment of this mouse model. The peak level of plasma CPK was

over 10,000 U/L at 4 days of drug co-administration. Mb in urine and kidney and cytoplasmic vacuolization in kidney were observed. Thus, it is assumed that rhabdomyolysis-induced AKI was triggered by Mb that leaked from skeletal muscle, as demonstrated in our mouse model (Matsubara et al., 2018). For decades, the rodent AKI model has been provided exclusively by kidney ischemia-reperfusion and by heavy metal or glycerol administration. In addition, excessive stress on the skeletal muscle due to intense exercise increases blood Mb level (Panizo *et al.*, 2015). It is well known that a decreased GSH level lowers the threshold for cellular oxidative stress, and cytotoxicity is likely to occur (Poprac *et al*., 2017). From these backgrounds, we assumed that severe skeletal muscle disorder is caused only by the GSH depletion treatment, and then AKI is induced due to the leaked Mb.

Our preliminary study was conducted under various administration conditions of BSO. Plasma CPK level did not increase with once-a-day dosing of BSO (1000 mg/kg, *i.p.*) up to 10 days (data not shown). BSO was treateded twice a day for 7 days, resulting in severe skeletal muscle injury (Fig 1). As for the dosing amount of BSO to mice, a commonly used 30 mM in drinking water (Watanabe et al., 2003) is approximately equivalent to daily *i.p.* administration in this study. GSH levels in skeletal muscle are decreased to 5% of the control level in mice by the drinking water method (Watanabe et al., 2003), and to 4% to 6% of total GSH in this study (Fig 5). Maximum depletion of hepatic GSH level occurred 4-6 hr after *i.p.* administration of BSO (1600 mg/kg), and after 15 hr, GSH content had returned to 83% of control level in mice (Drew and Miners, 1984). On the other hand, maximum depletion of GSH in the kidney (33% of control) occurred as early as 1 hr after BSO administration (1600 mg/kg), and at 15 hr after, kidney GSH levels were 53% of control level (Drew and Miners, 1984). Taking together, 12 hr interval for BSO administration method was adopted in the present

study.

Kang et al. (2014) reported that male C57BL/6J mice are more susceptible to renal ischemic injury compared with females of C57BL/6J mice. In this preliminary study, male and female C57BL/6J mice were compared. Male C57BL/6J mice demonstrated higher CPK level than females C57BL/6J mice (data not shown), thus, male mice were used in this study.

As a diagnostic index of clinical rhabdomyolysis, serum CPK and AST levels and the presence of muscle pain and myoglobinuria are adopted (Bagley et al., 2007, Hess et al., 1964; Reha et al., 1989; Zutt et al., 2014). Among them, serum CPK is the most important, and more than 10 times of the normal level (~2000 U/L) is regarded as the diagnostic criteria. In the present study, a noteworthy increase of CPK value exceeding 350,000 in particular indicated rhabdomyolysis (Fig. 1). Enzyme activities of antioxidant enzymes, such as glutathione peroxidase and glutathione reductase in the sleletal muscle are approximately 10-fold lower than those in the liver in a normal-state mouse (Leeuwnburgh et al., 1997), suggesting a low detoxification ability in the sleletal muscle. In addition, long-term BSO treatment causes mitochondrial damage in skeletal muscle (Mårtensson et al., 1989), suggesting the low capacity to scavenge reactive oxygen species, and easily causes cytotoxicity. This is inferred as the pathogenic mechanism of GSH depletion-induced rhabdomyolysis.

In recent years, circulating miRNA in plasma has become recognized as a highly sensitive and organ disorder-specific biomarker (Miyachi et al., 2010). Expression levels of miR-206-3p (skeletal muscle-specific) and miR-133b-3p (muscle and myocardium-specific) in plasma correlated significantly with serum CPK level in drug-induced rhabdomyolysis mouse model (Matsubara et al., 2018), suggesting skeletal muscle-specific injury in the present study. To support the data, expression

levels of miR-208-3p (myocardium-specific) (Ji et al., 2009) showed no change (data not shown). The expression level of miR-122-5p (liver-specific) (Bala et al., 2012) in plasma demonstrated no significant changes (Fig. 4B), indicating that the increased ALT level in the present study is not derived from hepatic injury. The increased ALT level will be dereived from sleletal muscle (Cotgreave et al., 2002). Unfortunately, there are no established miRNA biomarkers for kidney-specific injury.

The mechanism of rhabdomyolysis-induced AKI is proposed as follows: the skeletal muscle cell membrane is injured, Mb in skeletal muscle leaks into the blood, Mb accumulates in the kidney cells, and oxidative stress-induced kidney injury caused via Mb redox cycling generates oxidized lipids. These oxidized lipids propagate renal tissue injury (Boutaud and Roberts, 2011; Nara et al., 2016). Thus, Mb leaked from skeletal muscle is known to be a key mediator for AKI. Mb concentrations in human normal serum and urine are 30 to 80 ng/mL and 3 to 20 ng/mL, respectively. Generally, when Mb in the human plasma exceeds 15,000 ng/mL (1.5 mg/dL), it appears in the urine and becomes myoglobinuric (Petejova et al., 2014), turning urine brown. In this study, plasma and urine Mb levels peaked on day 7 and 8, respectively (Fig 2). Mb was deposited in renal tubule cells, and cytoplasmic vacuolization was observed in the proximal renal tubule. Therefore, it is considered that this study shows rhabdomyolysis-induced myoglobinuric AKI.

Rhabdomyolysis-induced myoglobinuric AKI accounts for 10% to 40% (Beetham, 2000) or 15% (Boutaud and Roberts, 2011) of all clinical cases of AKI. AKI is generally diagnosed by the daily increase of plasma BUN level greater than 10 mg/dL/day and plasma CRE level greater than 0.5 mg/dL/day (Edelstein, 2008); thus, in the present study (Fig 3), it is considered that AKI can be diagnosed on day 8.

In our previous studies (Higuchi *et al*., 2011; Kobayashi *et al*., 2009), we confirmed

that the expression profiles of mRNA and protein were similar for the interleukins, chemokines and stress- and inflammation-related proteins. Thus, changes in the mRNA expression levels were mainly investigated in the present study.

As for the liver, plasma ALT levels showed an upward trend from day 5. However, the plasma level of miR-122-5p (a biomarker for liver specific expression with very high sensitivity) was not increased (Fig. 4); thus, the elevated ALT is thought to be derived from the severely damaged skeletal muscle, not from the liver. Hepatic Ho-1 mRNA expression level was moderately increased (Fig 4C), which may be due to the GSH depletion-induced oxidative stress as suggested by Ito et al. (1997).

The expression level of representative renal injury biomarkers (Vanmassenhove et al., 2013; Haase-Fieltz et al., 2009), such as Lcn2/Ngal and Kim-1 renal mRNA and KIM-1 urine protein, was significantly increased on day 8 (Fig 3). However, it is reported that Lcn2/Ngal mRNA in kidney is significantly increased in the very early stage of lipopolysaccharide (LPS)-induced AKI in rats (Han et al., 2012) and cisplatin-induced AKI in humans (Gaspari et al., 2010). In addition, expression changes of Kim-1 and Tnfα mRNAs are very early biomarkers of cyclosporine A-induced AKI in rats (Carlos et al., 2014), and Il-6 is also an early biomarker of LPS-induced AKI in rats (Han et al., 2012). The onset time and pathological changes of AKI in the drug/chemical-induced direct AKI models differ from those of the present AKI model, in which the biomarkers increase shortly after the drug/chemical administration; further, lesions consisting of epithelial swelling and immune cell recruitment are observed, but no Mb involvement was reported in the drug/chemical-induced direct AKI models. Actually, in this study, the Lcn2/Ngal, Kim-1, Il-6, and Ho-1 mRNAs were significantly increased on day 8 (Supplemental figure 1), suggesting that AKI has not been sufficiently developed until day 7. There is a possibility that an AKI screening system that can use the late stage

onset can be devised.

Regarding the muscle-specific injury in this study, one of the reasons for it is that the detoxification ability in the sleletal muscle is low because all antioxidant enzyme activities are approximately 10-fold lower than those in the liver in a normal state in rodents (Leeuwnburgh et al., 1997), as mentioned previously. However, there is no evidence for a GSH replenishment ability under stress conditions in the skeletal muscle. Fisher-Wellman *et al*. (2013) reported that pyruvate dehydrogenase complex (PDC) is a key source of hydrogen peroxide within skeletal muscle mitochondria under conditions of depressed GSH redox buffering integrity. With a decreasing level of GSH, a release of the flux of hydrogen peroxide diffusing out of the mitochondrial matrix was observed (Fisher-Wellman et al., 2013). The critical mechanism underlying the development of rhabdomyolysis and subsequent onset of AKI with GSH-depletion condition can be found in future research.

In the present study, an AKI mouse model was established by the GSH depletion treatment in the normal mouse. This mouse model can be one of the new AKI models, and also would be useful for predicting potential AKI risks in non-clinical drug development.

Conflict of interest

None of the authors have any conflicts of interest related to this manuscript.

Supplementary data

Supplementary data related to this article can be found, in the online version.

REFERENCES

Ames, B. N., Shigenaga, M. K., & Hagen, T. M. (1993). Oxidants, antioxidants, and the degenerative diseases of aging. *Proceeding of the National Academy of Sciences of the United States of America*, 90, 7915–7922.

Bagley, W. H., Yang, H., & Shah, K. H. (2007). Rhabdomyolysis. *Internal and Emergency Medicine,* 2, 210–218. http://dx.doi.org/10.1007/s11739−007−0060−8

Bala, S., Petrasek, J., Mundkur, S., Catalano, D., Levin, I., Ward, J., … K., Szabo, G. (2012). Circulating microRNAs in exosomes indicate hepatocyte injury and inflammation in alcoholic, drug-induced, and inflammatory liver diseases. *Hepatology* 56, 1946–1957. http://dx.doi.org/10.1002/hep.25873

Beetham, R. (2000). Biochemical investigation of suspected rhabdomyolysis. *Annals of Clinical Biochemistry*, 37, 581–587. http://dx.doi.org/10.1258/0004563001899870

Boutaud, O., & Roberts, L. J. (2011). Mechanism-based therapeutic approaches to rhabdomyolysis-induced renal failure. *Free Radiccal Biology and Medicine*, 51, 1062–1067. http://dx.doi.org/10.1016/j.freeradbiomed.2010.10.704

Carlos, C. P., Sonehara, N. M., Oliani, S. M., & Burdmann, E. A. (2014). Oredictiveusefulness of urinry biomarkers for the identification of cyclosporine A-induced nephrotoxicity in rat model. *PLoS One,* 9, e103660. http://dx.doi.org/10.1371/journl.pone.0103660

Cotgreave, I. A., Goldschmidt, L., Tonkonogi, M., & Svensson, M. (2002). Differentiation-specific alterations to glutathione synthesis in and hormonally stimulated release from human skeletal muscle cells. *Federation of American Societies for Exprimental Biology Journal,* 16, 435–437. http://dx.doi.org/10.1096/fj01-0685fje

Drew, R., & Miners, J. O. (1984). The effects of buthionine sulphoximine (BSO) on glutathione depletion and xenobiotic biotransformetion. *Biochemical Pharmacology* 33, 2989-2994.

Edelstein, C. L. (2008). Biomarkers of acute kidney injury. *Advances in Chronic Kidney Disease,* 15, 222–234. http://dx.doi.org/10.1053/j.ackd.2008.04.003

Fisher-Wellman, K. H., Gilliam, L. A., Lin, C. T., Cathey, B. L., Lark, D. S. & Neufer, P. D. (2013). Mitochondrial glutathione depletion reveals a novel role for the pyruvate dehydrogenase complex as a key H_2O_2-emitting sourse under conditions of nutrient overload. *Free Radiccal Biology and Medicine*, 65, 1201–1208. http://dx.doi.org/10.1016/j.freeradbiomed.2013.09.008

Gaspari, F., Cravede, P., Mandala, M., Perico, N., de leon F.R., Stucchi, N., … Ruggenanti, P. (2010). Predicting cisplatin-indued acute kidney injury by urinary neutrophil gelatinase-associated lipocalin excretion: a pilot prospective case-control study. *Nephron Clinical Practice*, 115, 154–160. http://dx.doi.org/10.1159/000312879

Griffith, O. W. (1982). Mechanism of action, metabolism, and toxicity of buthionine sulfoximine and its higher homologs, potent inhibitors of glutathione synthesis. *The Journal of Biological Chemistry,* 257, 13704–13712.

Haase-Fielitz, A., Bellomo, R., Devarajan, P., Bennett, M., Story, D., Matalanis, G., … Haase, M. (2009). The predictive performance of plasma neutrophil gelatinase-associated lipocalin (NGAL) increases with grade of acute kidney injury. *Nephrology Dialysis Transplantation,* 24, 3349–3354. http://dx.doi.org/10.1093/ndt/gft234

Han, M., Li, Y., Liu, M., Li, Y., & Cong, B. (2012). Renal neutrophil gelatinase associated lipocalin expression in lipopolysaccharide-induced acute kidney injury

in the rat. *BMC Nephrology*, 13, 25. http://dx.doi.org/10.1186/1471-2369-13-25

Hess, J. W., Macdonald, R. P., Frederick, R. J., Jones, R. N., Neely, J., & Gross, D. (1964). Serum creatine phosphokinase (CPK) activity in disorders of heart and skeletal muscle. *Annals of Internal Medicine,* 61, 1015–1028.

Higuchi, S., Kobayashi, M., Yoshikawa, Y., Tsuneyama, K., Fukami, T., Nakajima, M., & Yokoi, T. (2011). IL-4 mediates dicloxacillin-induced liver injury in mice. *Toxicology Lettres,* 200, 139-145. http://dx.doi.org/10.1016/j.toxlet.2010.11.006

Iida, A, Sasaki, E., Yano, A., Tsuneyama, K., Fukami, T., Nakajima, M., & Yokoi, T. (2015). Carbamazepine-induced liver injury requires CYP3A-mediated metabolism and glutathione depletion in rats. *Drug Metabolism and Disposition*, 43, 958–968. http://dx.doi.org/10.1124/dmd.115.063370

Ito, K., Yano, T., Hagiwara, K., Ozaha, H., & Horikawa, S. (1997). Effects of vitamin E deficiency and glutashione depletion on stress protein heme oxygenase 1 mRNA expression in rat liver and kidney. *Biochemical Pharmacology*, 54, 1081–1086. http://dx.doi.org/

Iwamura, A., Watanabe, K., Akai, S., Nishinosono, T., Tsuneyama, K., Oda, S., … Yokoi, T. (2016). Zomepirac acyl glucuronide is responsible for zomepirac-induced acute kidney injury in mice. *Drug Metabolism and Disposition*, 44, 888–896. http://dx.doi.org/10.1124/dmd.116.069575

Ji, X., Takahashi, R., Hiura, Y., Hirokawa, G., Fukushima, Y., & Iwai, N. (2009). Plasma miR-208 as a biomarker of myocardial injury. *Clinical Chemistry,* 55, 1944–1949. http://dx.doi.org/10.1373/clinchem.2009.125310.

Kang, K. P., Lee, J. E., Lee, A. S., Jung, Y. J., Kim, D., Lee, S.,… Park, S. K. (2014). Effect of gender differences on the regulation of renal ischemia-reperfusion-induced inflammation in mice. *Molecular Medicine Reports,*

9, 2061-2068. http://dx.doi.org/ 10.3892/mmr.2014.2089.

Kiyosawa, N., Ito, K., Sakuma, K., Niino, N., Kanbori, M., Yamoto, T.,… Matsunuma, N. (2004). Evaluation of glutathione deficiency in rat livers by microarray analysis. *Biochemical Pharmacology,* 68, 1465–1475. http://dx.doi.org/10.1016/j.bcp.2004.05.053

Kiyosawa, N., Uehara, T., Gao, W.-H., Omura, K., Hirode, M., Shimizu, T.,,,,,Urushidani, T. (2007). Identification of glutathione depletion-responsive genes using phorone-treated rat liver. The Journal of Toxicological Sciences 32, 469–486.

Kobayashi, E., Kobayashi, M., Tsuneyama, K., Fukami, T., Nakajima, M., & Yokoi, T. (2009). Halothane-induced liver injury is mediated by interleukin-17 in mice. *Toxicological Sciences,* 111, 302-310. http://dx.doi.org/10.1093/toxsci/kfp165

Leeuwenburgh, G., Hollander, J., Leichtwies, S. Griffiths, M., Gore, M., & Ji, I. I. (1997). Adaptations of glutathione antioxidant system to endurance training are itssue and muscle fiber specific. *The American Journal of Physiology*, 272. 363–369. http://dx.doi.org/10.1152/ajpregu.1997.272.1.R363

Lu, S. C. (1999). Regulation of hepatic glutathione synthesis: current concepts and controversies. *Federation of American Societies for Exprimental Biology Journal,* 13, 1169–1183.

Lu, S. C. (2013). Glutathione synthesis. *Biochimica et Biophysica Acta*, 1830, 3143-3153. http://dx.doi.org/10.1016/j.bbagen.2012.09.008

Mårtensson, J., & Meister, A. (1989). Mitochondrial damage in muscle occurs after marked depletion of glutathione and is prevented by giving glutathione monoester. *Proceeding of the National Academy of Sciences of the United States of America*, 86, 471–475.

Matsubara, A., Oda, S., Akai, S., & Yokoi, T. (2018). Establishment of a drug-induced rhabdomyolysis mouse model by co-administration of ciprofloxacin and atorvastatin. *Toxicology Letters,* 291, 184–193. http://dx.doi.org/10.1016/j.toxlet.2018.04.016

Miyachi, M., Tsuchiya, K., Yoshida, H., Yagyu, S., Kikuchi, K.,… Hosoi, H. (2010). Circulating muscle-specific microRNA, miR-206, as a potential diagnostic marker for rhabdomyosarcoma. *Biochemical and Biophysical Research Communications,* 400, 89–93. http://dx.doi.org/10.j.bbrc.2010.08.015

Nara, A., Yajima, D., Nagasawa, S., Abe, H., Hoshioka, Y. & Iwase, H. (2016). Evaluations of lipid peroxidation and inflammation in short-term glycerol-induced acute kidney injury in rats. *Clinical and Experimental Pharmacology and Physiology*, 43, 1080-1086. http://dx.doi.org/10.1111/1440-1681.12633

Panizo, N., Rubio-Navarro, A., Amaro-Villalobos, J. M., Egido, J., & Moreno, J.A. (2015). Molecular mechanisms and novel therapeutic approaches to rhabdomyolysis-induced acute kidney injury. *Kidney Blood Press Research,* 40, 520–532. http://dx.doi.org/10.1159/000368528

Poprac, P., Jomova, K., Simunkava, M., Kollar, V., Rhodes, C. J., & Valko, M. (2017). Targeting free radicals in oxidative stres-related human diseases. *Trends Phamacological Sciences*, 38, 592–607. http://dx.doi.org/10.1016/j.tips.2017.04.005

Petejova, N., & Martinek, A. (2014). Acute kidney injury due to rhabdomyolysis and renal replacement therapy: a critical review. *Critical Care,* 18, 224–231. http://dx.doi.org/10.1186/cc13897

Reha, W. C., Mangano, F. A., Zeman, R. K., & Pahira, J. J. (1989). Rhabdomyolysis: need for high index of suspicion. *Urology,* 34, 292–295.

Shirai, Y., Oda, S., Makino, S., Tsuneyama, K., & Yokoi, T. (2017). Establishment of a mouse model of enalapril-induced liver injury and investigation of the pathogenesis. *Laboratory Investigation,* 97, 833–842. http://dx.doi.org/10.1038/labinvest.2017.22

Vanmassenhove, J., Vanholder, R., Nagler, E., & Van Biesen, W. (2013). Urinary and serum biomarkers for the diagnosis of acute kidney injury: An in-depth review of the literature. *Nephrology Dialysis Transplantation,* 28, 254–273. http://dx.doi.org/10.1093/ndt/gfs380

Vaziri, N. D., Wang, X. Q., Oveisi, F., & Rad, B. (2000). Induction of oxidative stress by glutathione depletion causes severe hypertension in normal rats. *Hypertension,* 36, 142–146. http://dx.doi.org/

Watanabe, T., Sagisaka, H., Arakawa, S., Shibaya, Y., Watanabe, M., Igarashi, I.,… Manabe, S. (2003). A novel model of continuous depletion of glutathione in mice treated with L-buthionine (*S,R*)-sulfoximine. *The Journal of Toxicological Sciences,* 28, 455–469.

Wu, G., Fang, Y-A., Yang, S., Lupton, J.R., & Turner, N.D. (2004). Glutathione metabolism and its implications for health. *The Journal of Nutrition,* 134, 489–492. http://dx.doi.org/10.1093/jn/134.3.489

Zutt, R., van der Kooi, A. J., Linthorst, G. E., Wanders, R. J. A., & de Visser, M. (2014). Rhabdomyolysis: Review of the literature. *Neuromuscular Disorders*, 24, 651–659. http://dx.doi.org/10.1016/j.nmd.2014.05.005

TABLE 1

miRNAs used in this study.

Gene	Sequence (5' to 3')	Tissue specificity	miRbase accession number	Reference Pubmed ID
mmu-miR-206-3p	UGGAAUGUAAGGAAGUGUGUGG	Skeletal muscle	MIMAT0000239	18381085
mmu-miR-133b-3p	UUUGGUCCCCUUCAACCAGCUA	Skeletal muscle Heart	MIMAT0000769	17468766
mmu-miR-208a-3p	AUAAGACGAGCAAAAAGCUUGU	Heart	MIMAT0000520	25092230
mmu-miR-122-5p	UGGAGUGUGACAAUGGUGUUUG	Liver	MIMAT0000246	29235390
ath-miR159a	UUUGGAUUGAAGGGAGCUCUA		MIMAT0000177	

TABLE 2

Sequences of mRNA primers used for real-time RT-PCR analyses.

Gene		Sequence (5' to 3)	NCBI accession
Gapdh	F	AAATGGGGTGAGGCCGGT	NM_001289726.1
	P	ATTGCTGACAATCTTGAGTGA	
Ho-1	F	GACACCTGAGGTCAAGCACA	NM_010442.2
	P	ATCACCTGCAGCTCCTCAAA	
Il-1β	F	GTTGACGGACCCCAAAAGAT	NM_008361.4
	P	CACACACCAGCAGGTTATCA	
Il-6	F	CCATAGCTACCTGGAGTACA	NM_031168.2
	P	GGAAATTGGGGTAGGAAGGA	
Kim-1	F	AGATTCCCACACGTCCTCCAA	NM_134248.2
	P	TGTCACCTCAGCTGTTGTCTC	
Mcp-1	F	TGTCATGCTTCTGGGCCTG	NM_011333.3
	P	CCTCTCTCTTGAGCTTGGTG	
Lcn2/Ngal	F	ATGTCACCTCCATCCTGGTC	NM_008491.1
	P	CCTGTGCATATTTCCCAGAGT	
Tnfα	F	TGTCTCAGCCTCTTCTCATTCC	NM_013693.3
	P	TGAGGGTCTGGGCCATAGAAC	
Xirp1	F	TTACTCAAGGCAGCATCAGG	NM_011724.3
	P	TTGAGTTGGGTGGTCAGGAT	

F: forward primer, R: reverse primer

FIGURE LEGENDS

FIGURE 1. Effects of BSO treatment on plasma CPK, AST, and miRNA levels of miR-206-3p and miR-133b-3p, and muscle Xirp1 and Ho-1 mRNA expression level, and histological examination of skeletal muscle in C57BL/6J mice.

Time-dependent changes of plasma CPK and AST were measured 12 hours after the second daily BSO treatment (A and B). miRNAs, mRNAs, and histological data were measured 12 hours after the last BSO treatment on day 7. The relative plasma miRNAs levels were measured using real-time RT-PCR and normalized to that of ath-miR159a (spike in control). The fold induction of the miRNA level is shown compared with that of day 0 control group (C and D). The relative expression levels of the muscle Xirp 1 (E) and Ho-1 (F) mRNA were measured using real-time RT-PCR and normalized to that of Gapdh mRNA. Skeletal muscle sections were stained with H&E (G). Red, blue, and green arrows show muscle fiber degeneration, necrosis, and satellite cells, respectively. Scale bars are equal to 100 μm. The data are shown as the means ± SEM (n = 4-5). The differences of plasma CPK and AST compared with that of the saline-treated control group were considered significant at *$p < 0.05$, **$p < 0.01$ and ***$p < 0.001$, and with the day 0 control group was $^{\dagger\dagger\dagger}p<0.001$ by Dunnett's test, and with the day 8 saline-treated control group was $^{\#\#}p<0.01$ and $^{\#\#\#}p<0.001$ by Student's t-test.

FIGURE 2. Effect of BSO treatment on Mb concentration in plasma and urine, and immunohistochemical examination of kidney.

Time-dependent changes of Mb level in plasma and urine were measured by ELISA 12 hours after the second daily BSO treatment (A and B). Urine was collected from the

bladder directly at the time of the dissection. The data are shown as the means ± SEM (n = 4-5). Differences compared with saline-treated control group were considered significant at *p<0.05, **p<0.01 by Dunnett's test. (C) Kidney was collected 12 h after the last BSO treatment. Mb was immunostained in the kidney section. Red arrow shows renal casts. Scale bar = 100 μm.

FIGURE 3. Effects of BSO treatment on plasma and urine biochemical scores, and kidney mRNA expression levels, and histological examination of kidney in C57BL/6J mice.

Time-dependent changes of plasma BUN and CRE, and urinary CRE were measured 12 hours after the second daily BSO treatment (A, B, and C). The relative expression levels of kidney Lcn2/Ngal (D), Kim-1 (E), Ho-1 (G), Il-6 (H), Il-1b (I), Tnfα (J), and Mcp-1 (K) were measured 12 hours after the last BSO treatment using real-time RT-PCR and normalized to that of Gapdh mRNA. The fold induction of the mRNA level is shown compared with day 0 control group. KIM-1 protein level in urine was measured by ELISA (F). Kidney sections were stained with H&E (L). Red and blue arrows show renal tubular obstruction and vacuolization, respectively. Scale bar = 100 μm. The data are shown as the means ± SEM (n = 4-5). The differences of plasma BUN and CRE and urine CRE compared with that of saline-treated control group were considered significant at *p < 0.05, **p < 0.01 and ***p < 0.001 (A to C), and with the day 0 group was † p<0.05, †† p<0.05 by the Dunnett's test, and with the day 8 saline group $^{\#\#}$p<0.01 by Student's t-test (D to K).

FIGURE 4. Effects of BSO treatment on plasma ALT and miR-122-5p level and hepatic mRNA expression level of Ho-1 and Mcp-1.

Time-dependent change of plasma ALT was measured 12 hours after the second daily BSO treatment (A). The relative expression level of the plasma miR-122-5p was measured using real-time RT-PCR and normalized to that of ath-miR159a (spike in control). The fold induction of the miRNA level is shown compared with that of day 0 control group (B). The relative expression levels of the hepatic Ho-1 (C) and Mcp-1 (D) mRNA were measured using real-time RT-PCR and normalized to that of Gapdh mRNA. Data are shown as the means ± SEM (n = 4-5). The differences of plasma ALT compared with that of the saline-treated control group were considered significant at *p < 0.05, and ***p < 0.001. Differences in comparison to the day 0 group were considered significant at ††p<0.01 by the Dunnett's test, and with day 8 saline-treated control group $^{\#}$p<0.05 by Student's t-test.

FIGURE 5. Effects of BSO treatment on GSH contents in liver, kidney, and skeletal muscle.

(A) Total GSH, (B) GSH, and (C) GSSG contents and (D) GSH/GSSG ratio in the liver, kidney, and skeletal muscle were measured 12 hours after the last BSO treatment. Data are shown as the means ± SEM (n = 4-5). Differences in comparison to the day 0 group were considered significant at *p<0.05, **p<0.01 and ***p<0.001 by the Dunnett's test, and with the day 8 saline control group $^{\#}$p<0.05 and $^{\#\#\#}$p<0.001 by Student's t-test.

Figure 1

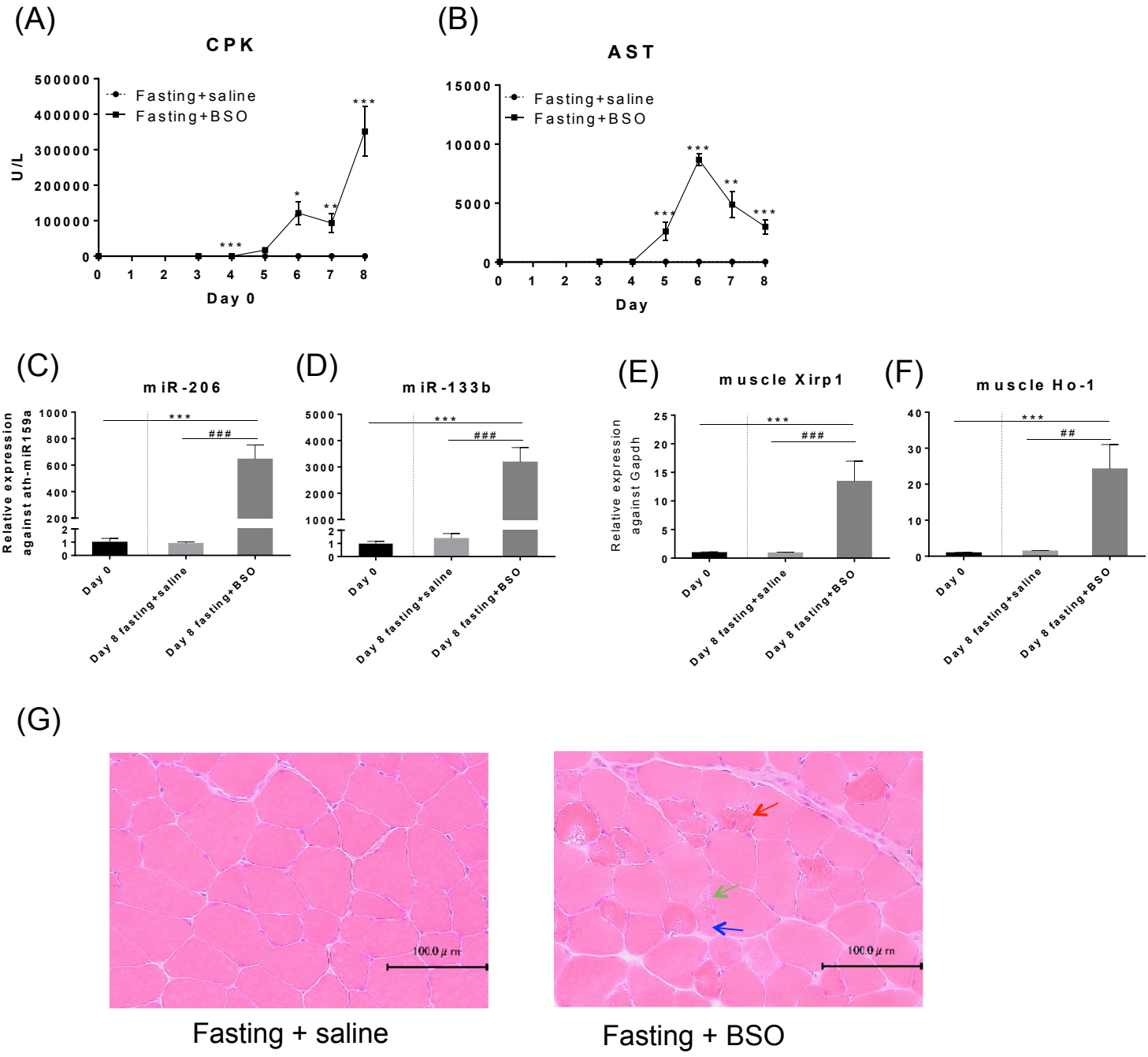
(A)
CPK
Fasting+saline
Fasting+BSO
U/L
Day 0
(B)
AST
Fasting+saline
Fasting+BSO
Day
(C)
miR-206
Relative expression against ath-miR159a
Day 0
Day 8 fasting+saline
Day 8 fasting+BSO
(D)
miR-133b
(E)
muscle Xirp1
Relative expression against Gapdh
(F)
muscle Ho-1
(G)
100.0 μm
Fasting + saline
Fasting + BSO

Figure 2

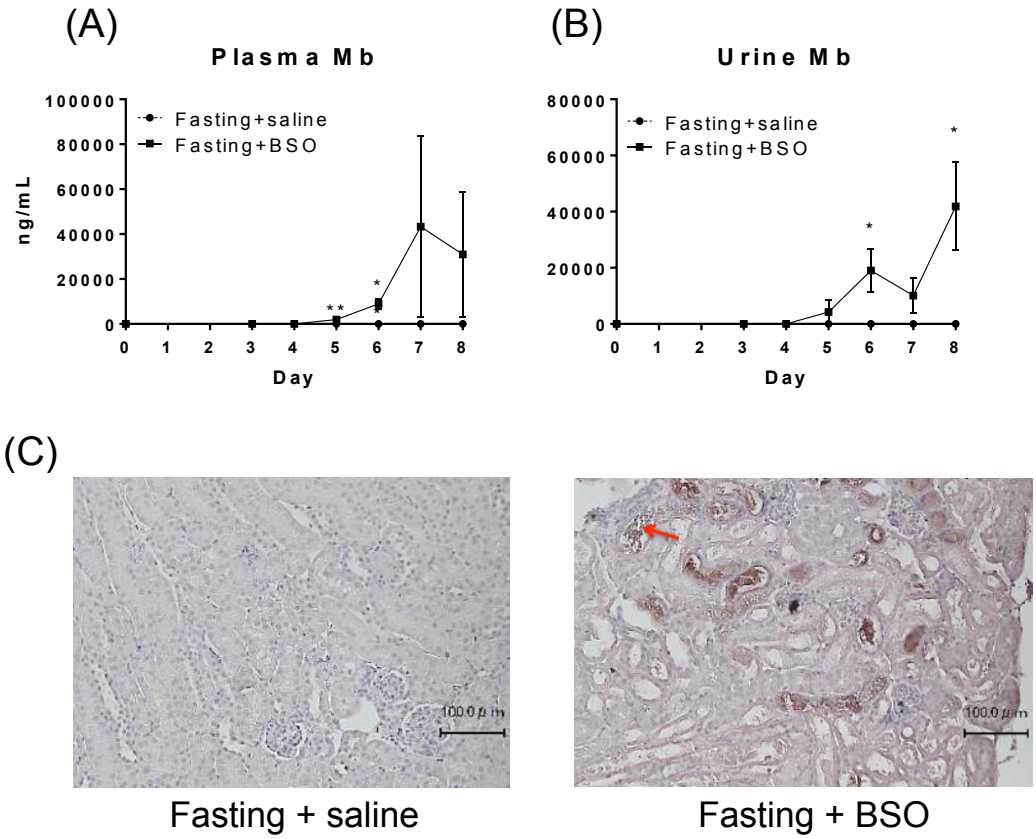
(A)
Plasma Mb
Fasting+saline
Fasting+BSO
ng/mL
Day
(B)
Urine Mb
Fasting+saline
Fasting+BSO
Day
(C)
100.0 µm
100.0 µm
Fasting + saline
Fasting + BSO

Figure 3

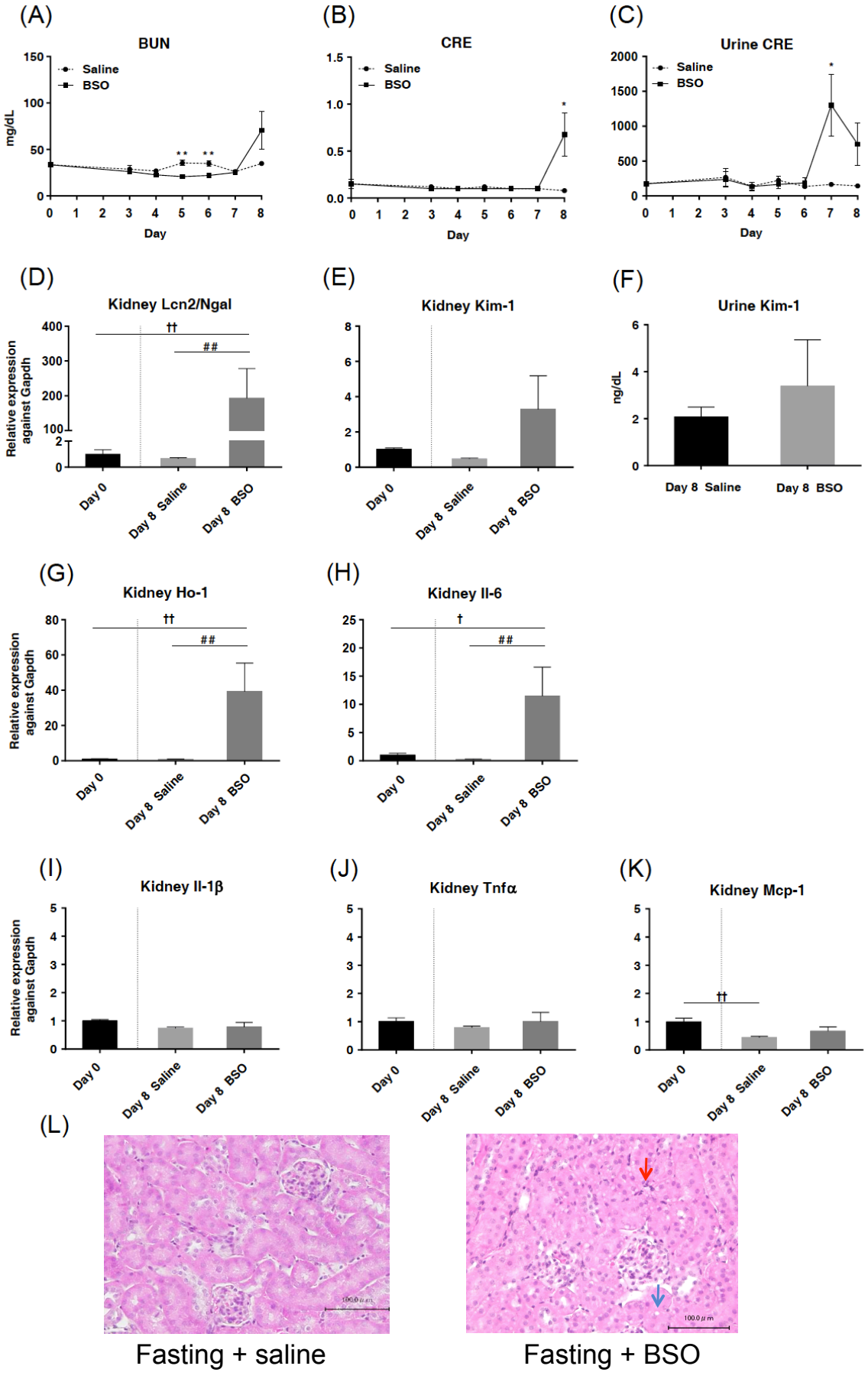
(A)
BUN
Saline
BSO
mg/dL
Day
(B)
CRE
Saline
BSO
Day
(C)
Urine CRE
Saline
BSO
Day
(D)
Kidney Lcn2/Ngal
Relative expression against Gapdh
Day 0
Day 8 Saline
Day 8 BSO
(E)
Kidney Kim-1
Day 0
Day 8 Saline
Day 8 BSO
(F)
Urine Kim-1
ng/dL
Day 8 Saline
Day 8 BSO
(G)
Kidney Ho-1
Relative expression against Gapdh
Day 0
Day 8 Saline
Day 8 BSO
(H)
Kidney Il-6
Day 0
Day 8 Saline
Day 8 BSO
(I)
Kidney Il-1β
Relative expression against Gapdh
Day 0
Day 8 Saline
Day 8 BSO
(J)
Kidney Tnfα
Day 0
Day 8 Saline
Day 8 BSO
(K)
Kidney Mcp-1
Day 0
Day 8 Saline
Day 8 BSO
(L)
Fasting + saline
Fasting + BSO

Figure 4

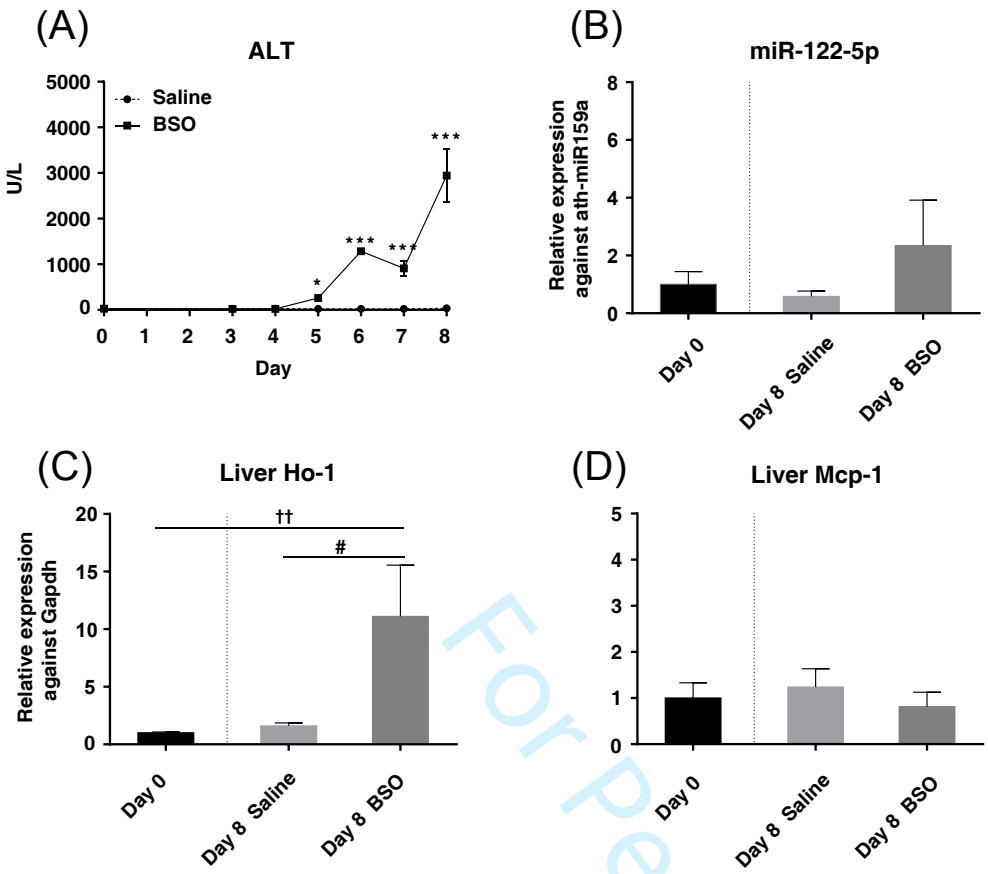

Figure 5

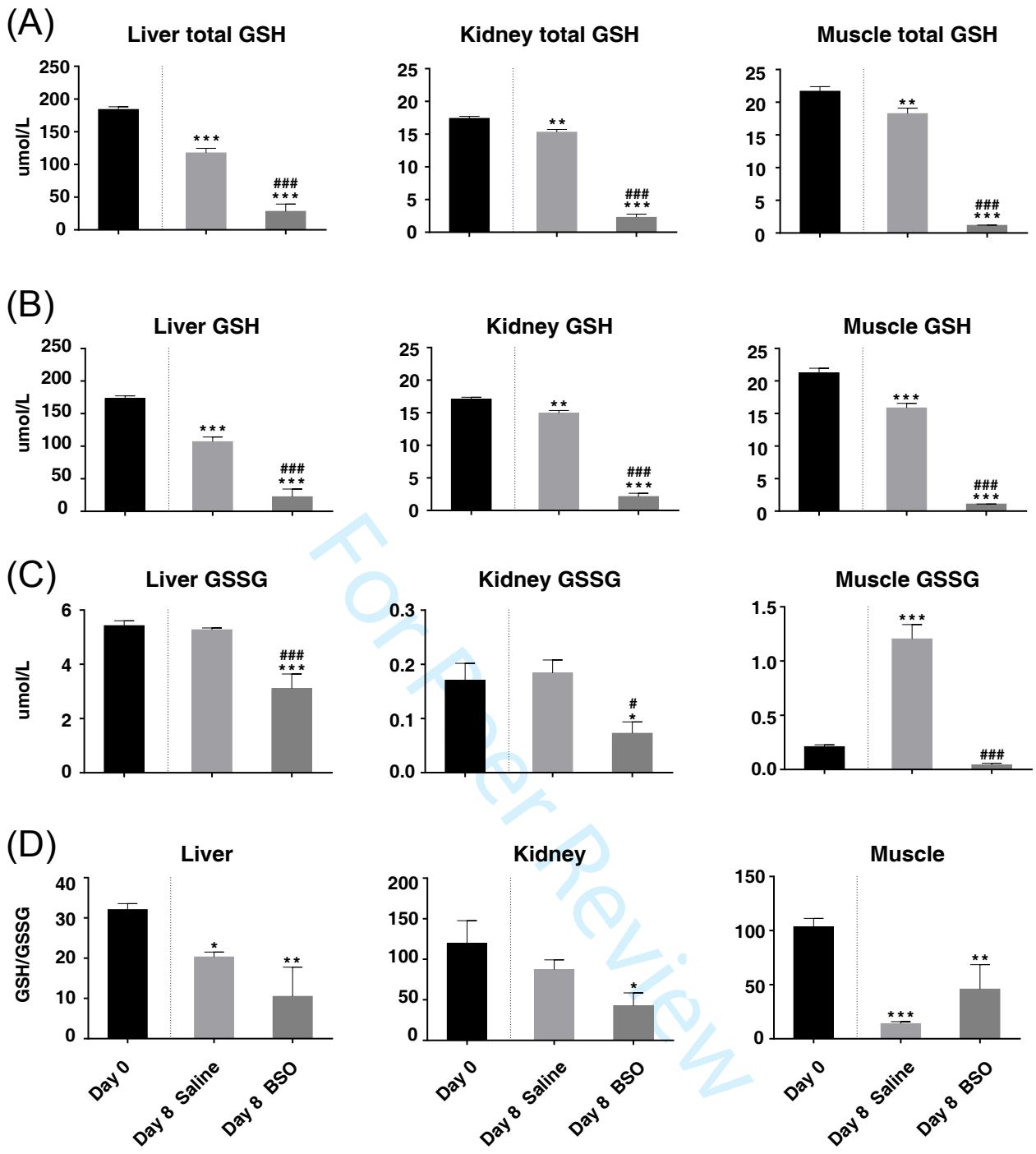

Supplemental figure 1

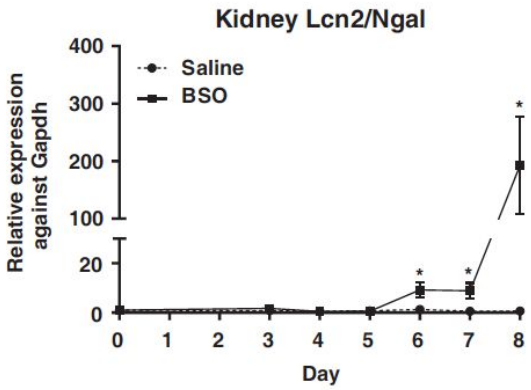

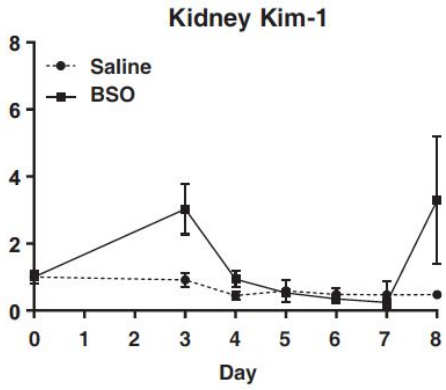

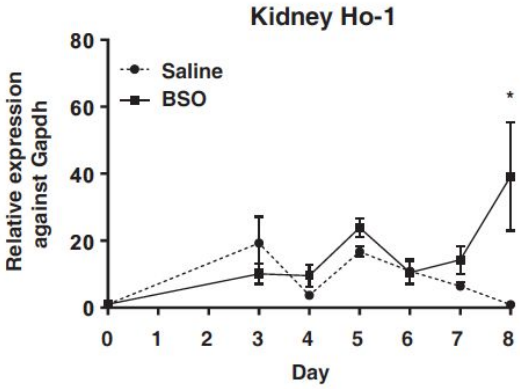

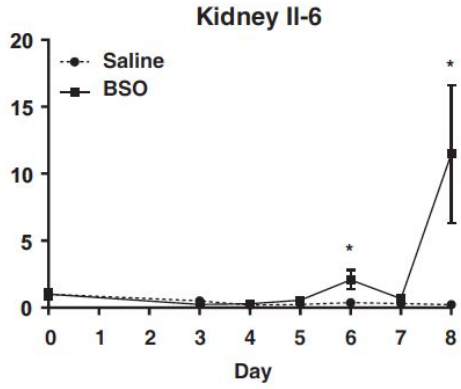

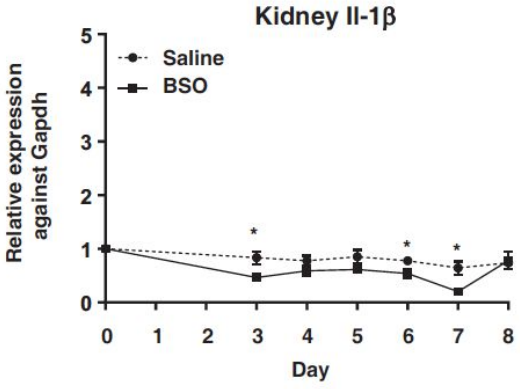

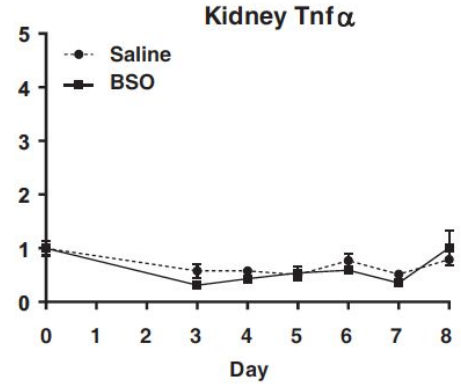

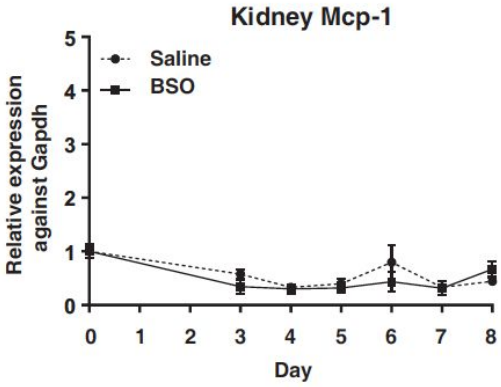

Supplemental figure 2

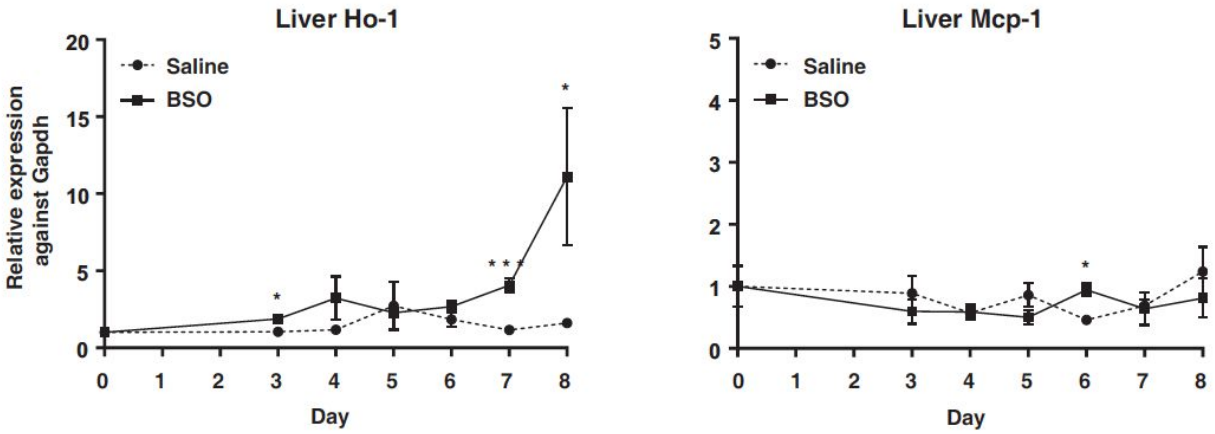

Legend for Supplementary Figures

Supplementary Figure 1

Time-dependent changes of the mRNA expression levels in kidney with or without BSO treatment.

Time-dependent changes of the mRNA expression levels in kidney were measured 12 hours after the second daily BSO treatment. The relative expression levels of kidney mRNA were measured using real-time RT-PCR and normalized to that of Gapdh mRNA. The data are shown as the means ± SEM (n = 4-5). Differences compared with saline-treated control group were considered significant at *p<0.05, and ***p<0.001 by Dunnett's t-test.

Supplementary Figure 2

Time-dependent changes of the mRNA expression levels in hepatic Ho-1 and Mcp-1 with or without BSO treatment.

Time-dependent changes of the expression level in hepatic Ho-1 and Mcp-1 were measured 12 hours after the second daily BSO treatment. The relative expression levels of hepatic Ho-1 and Mcp-1 mRNA were measured using real-time RT-PCR and normalized to that of Gapdh mRNA. The data are shown as the means ± SEM (n = 4-5). Differences compared with saline-treated control group were considered significant at *p<0.05, and ***p<0.001 by Dunnett's t-test.